1
What is a Pomeron?

Before the advent of the field theoretic approach (QCD), a good deal of progress had already been made in developing an understanding of the scattering of strongly interacting particles. This progress was founded on some very general properties of the scattering matrix. Regge theory provided a natural framework in which to discuss the scattering of particles at high centre-of-mass energies.

With the arrival of QCD much attention was diverted away from the 'old fashioned' approach to the strong interactions. Interest was re-ignited within the particle physics community with the arrival of colliders capable of delivering very large centre-of-mass energies (e.g. the HERA collider at DESY and the Tevatron collider at FNAL). For the first time physicists started to investigate in earnest the properties of QCD at high energies and compare them with the predictions of the Regge theory.

The high energy limit provides the arena in which the Regge properties of QCD can be studied. It is the meeting place of the 'old' particle physics with the 'new'. Since by 'old' we mean over 30 years ago it is necessary to commence our study of high energy scattering in QCD with an introduction to (or recap of) Regge theory. This chapter will contain a 'whistle-stop tour' of Regge theory and Pomeron phenomenology. We keep this to the minimum which will be required in order to follow the subsequent chapters and refer the interested reader to the literature (e.g. Collins (1977)) for further details.

1.1 Life before QCD

Before the development of QCD nobody dared to apply quantum field theory to the strong interactions. Instead, physicists tried

https://doi.org/10.1017/9781009290111.003 Published online by Cambridge University Press

to extract as much as possible by studying the consequences of a (reasonable) set of postulates about the S-matrix, whose abth element is the overlap between the *in*-state (free particles state as $t \to -\infty$), $|a\rangle$, and the *out*-state (free particles state as $t \to +\infty$), $|b\rangle$,

$$S_{ab} = \langle b_{out} \,|\, a_{in} \rangle.$$

Postulate 1:
The S-matrix is Lorentz invariant.

This means that it can be expressed as a function of the (Lorentz invariant) scalar products of the incoming and outgoing momenta. For two-particle to two-particle scattering,

$$a + b \to c + d,$$

these are most effectively described in terms of the Mandelstam variables, s, t, and u defined by

$$\begin{aligned} s &= (p_a + p_b)^2 \\ t &= (p_a - p_c)^2 \\ u &= (p_a - p_d)^2, \end{aligned}$$

as well as the four masses, m_a, m_b, m_c, m_d. The total energy of the system in the centre-of-mass frame is $\sqrt{s}$ and t is the square of the four-momentum exchanged between particles a and c and is related to the scattering angle. u is not an independent variable since by conservation of momentum we can show that[†]

$$s + t + u = m_a^2 + m_b^2 + m_c^2 + m_d^2.$$

We therefore write a two-particle to two-particle scattering amplitude as $\mathcal{A}(s, t)$, a function of s and t only (the amplitude also depends on the masses of the external particles).

For two-particle to n particle scattering processes there are $3n-4$ independent invariants.

Postulate 2:
The S-matrix is unitary:

$$S S^\dagger = S^\dagger S = \mathbb{1}.$$

[†] Throughout this book we work in the system of units $\hbar = c = 1$.

https://doi.org/10.1017/9781009290111.003 Published online by Cambridge University Press

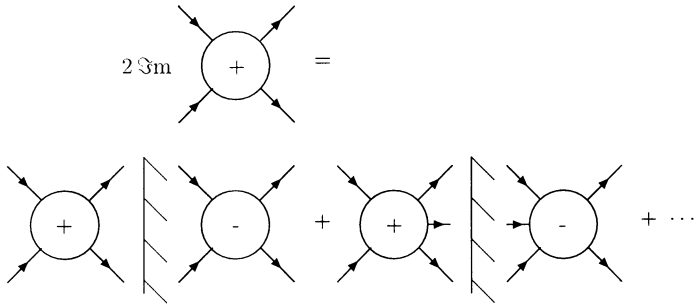

Fig. 1.1. The Cutkosky rules for a two-particle to two-particle amplitude. The shaded cut line denotes that the intermediate particles are on mass-shell whilst the + and − signs denote the amplitude and its hermitian conjugate respectively.

This is a statement of conservation of probability, i.e. the probability for an *in*-state to end up in a particular *out*-state, summed over all possible *out*-states, must be unity.

The scattering amplitude, $\mathcal{A}_{ab}$, for scattering from an *in*-state $|\, a\rangle$ to an *out*-state $|\, b\rangle$ is related to the S-matrix element by

$$S_{ab} = \delta_{ab} + i(2\pi)^4\delta^4\left(\sum_a p_a - \sum_b p_b\right)\mathcal{A}_{ab}$$

$((2\pi)^4\delta^4\left(\sum_a p_a - \sum_b p_b\right)\mathcal{A}_{ab}$ is often called the T-matrix element T_{ab} where $S = \mathbb{1} + iT$) and the unitarity of the S-matrix leads to the relation

$$2\Im\mathrm{m}\,\mathcal{A}_{ab} = (2\pi)^4\delta^4\left(\sum_a p_a - \sum_b p_b\right)\sum_c \mathcal{A}_{ac}\mathcal{A}^\dagger_{cb}. \qquad (1.1)$$

This gives us the Cutkosky (1960) rules, which allow us to determine the imaginary part of an amplitude by considering the scattering amplitudes of the incoming and outgoing states into all possible 'intermediate' states. These rules will be used extensively in later chapters. For the case of two-particle to two-particle scattering the Cutkosky rules are shown schematically in Fig. 1.1. Here the shaded 'cut' line means that the intermediate particles are taken to be on their mass-shell and an integral is performed over the phase space of the intermediate particles. The minus signs in the amplitudes on the right of the cuts mean that the hermi-

https://doi.org/10.1017/9781009290111.003 Published online by Cambridge University Press

tian conjugate is taken, i.e. the *in*- and *out*-states are interchanged and the complex conjugate is taken (in perturbation theory this implies that the sign of the $i\epsilon$ for each internal propagator is reversed).

An important special case of the Cutkosky rules is the **optical theorem**, which relates the imaginary part of the forward elastic amplitude, $\mathcal{A}_{aa}$, to the total cross-section for the scattering of the (two-particle) state, $|a\rangle$,

$$2\Im\mathrm{m}\mathcal{A}_{aa}(s,0) = (2\pi)^4 \sum_n \delta^4\left(\sum_f p_f - \sum_a p_a\right) |\mathcal{A}_{a\to n}|^2 = F\,\sigma_{\mathrm{tot}}, \tag{1.2}$$

where F is the flux factor (for $\sqrt{s}$ much larger than the masses of the incoming particles $F \approx 2s$).

Postulate 3:
The S-matrix is an analytic function of Lorentz invariants (regarded as complex variables), with only those singularities required by unitarity.

It can be shown that this 'analyticity' property is a consequence of causality, i.e. that two regions with a space-like separation do not influence each other.

Analyticity has a number of important and useful consequences. Combined with unitarity we are able to establish the existence of the s-plane singularity structure of the amplitude $\mathcal{A}(s,t)$ shown in Fig. 1.2, i.e. there are s-plane cuts with branch points corresponding to physical thresholds. These arise because the n-particle states must contribute to the imaginary part of the amplitude if s is greater than the n-particle threshold (see Eq.(1.1)). The imaginary part of the amplitude is

$$\Im\mathrm{m}A(s,t) = \frac{A(s,t) - A(s,t)^*}{2i}.$$

Below threshold there are no contributions to the imaginary part and so there exists a region on the real s-axis (around the origin) where the amplitude is purely real. This means that we can use the Schwarz reflection principle, which states that a function (of s) which is real on some part of the real s-axis satisfies

$$\mathcal{A}(s,t)^* = \mathcal{A}(s^*,t)$$

https://doi.org/10.1017/9781009290111.003 Published online by Cambridge University Press

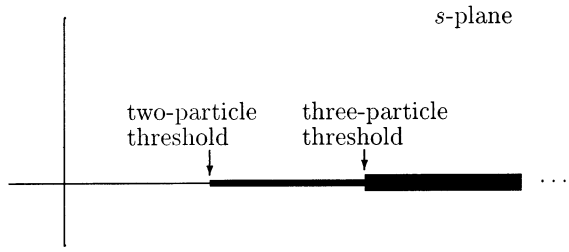

Fig. 1.2. The cuts on the positive real axis in the complex s-plane.

throughout its domain of analyticity. So, in order to have an imaginary part for real s above threshold, we need a cut along the real axis with branch point at the threshold energy.† Using the Schwarz reflection principle we can write

$$\Im\mathrm{m}A(s+i\epsilon,t) = \frac{A(s+i\epsilon,t) - A(s-i\epsilon,t)}{2i}$$

in the region where the amplitude is analytic, e.g. for real s and ϵ. This is non-zero for real s above threshold and allows us to define the imaginary part of the physical scattering amplitude above threshold as

$$\Im\mathrm{m}\,\mathcal{A}(s,t) = \frac{1}{2i}\lim_{\epsilon\to 0}\left[\mathcal{A}(s+i\epsilon,t) - \mathcal{A}(s-i\epsilon,t)\right]. \qquad (1.3)$$

The right hand side is called the **s-channel discontinuity** and is often denoted by $\Delta_s\mathcal{A}(s,t)$.‡ Analyticity also implies, as we shall shortly show, that there are cuts along the negative real axis.

A further consequence of analyticity is crossing symmetry. Consider the scattering process

$$a + b \to c + d, \qquad (1.4)$$

and write its amplitude as $\mathcal{A}_{a+b\to c+d}(s,t,u)$ (we have reinstated the variable u for the sake of symmetry but understand that this is *not* an independent variable). Now in the physical kinematic regime for the process (1.4) we have $s > 0$ and $t, u < 0$. Since the amplitude is an analytic function it may be analytically continued

† This is true for ≥ 2 particles in the intermediate state. For single particle production, i.e. a bound state of mass m, we have a pole at $s = m^2$.

‡ This corresponds to the definition of the physical scattering amplitude as the limit $\lim_{\epsilon\to 0} A(s+i\epsilon,t)$.

https://doi.org/10.1017/9781009290111.003 Published online by Cambridge University Press

to the region $t > 0$ and $s, u < 0$. This gives the amplitude for the t-channel process,

$$a + \bar{c} \to \bar{b} + d, \tag{1.5}$$

where $\bar{b}$, $\bar{c}$ mean the antiparticles of particles b and c respectively. Thus we have

$$\mathcal{A}_{a+\bar{c}\to\bar{b}+d}(s,t,u) = \mathcal{A}_{a+b\to c+d}(t,s,u) \tag{1.6}$$

and similarly for the u-channel process,

$$a + \bar{d} \to \bar{b} + c, \tag{1.7}$$

we have

$$\mathcal{A}_{a+\bar{d}\to\bar{b}+c}(s,t,u) = \mathcal{A}_{a+b\to c+d}(u,t,s). \tag{1.8}$$

Since the amplitude for the t-channel and u-channel processes also have imaginary parts and consequently physical thresholds, there must be cuts along the real positive t and u axes with branch points at these thresholds. Now $u = \sum_i m_i^2 - s - t$, so that the existence of a threshold at $u = u_{th}$ for positive u (at fixed t) means that as well as a branch point at positive $s = s_{th}^+$ corresponding to the physical threshold for the s-channel process, the amplitude, $\mathcal{A}(s,t)$ must have a cut along the negative real s-axis with a branch point at $s = s_{th}^- = \sum_i m_i^2 - t - u_{th}$.

The next important consequence of analyticity which we shall make use of is that it enables us to reconstruct the real part of an amplitude from its imaginary part using dispersion relations. We refer to the standard texts on mathematical physics for those readers unfamiliar with dispersion relations (e.g. Mathews & Walker (1970)).

The Cauchy integral formula allows us to write

$$\mathcal{A}(s,t) = \frac{1}{2\pi i} \oint_C \frac{\mathcal{A}(s',t)}{(s'-s)}\, ds',$$

where C is a contour that does not enclose any of the singularities of $\mathcal{A}$. Such a contour is shown in Fig. 1.3. It goes around the cuts along the positive and negative real axes and around the semicircles at infinity. The contributions to the contour integral from

https://doi.org/10.1017/9781009290111.003 Published online by Cambridge University Press

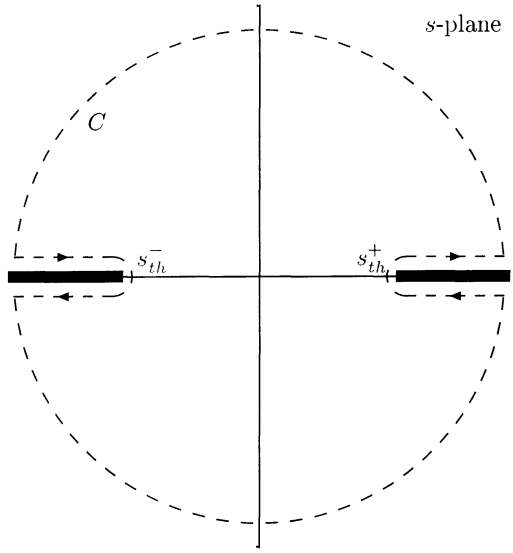

Fig. 1.3

the parts that surround the cuts are

$$\int_{s_{th}^+}^{\infty} ds' \frac{\mathcal{A}(s'+i\epsilon,t)}{(s'-s)} + \int_{\infty}^{s_{th}^+} ds' \frac{\mathcal{A}(s'-i\epsilon,t)}{(s'-s)}$$
$$+ \int_{-\infty}^{s_{th}^-} ds' \frac{\mathcal{A}(s'+i\epsilon,t)}{(s'-s)} + \int_{s_{th}^-}^{-\infty} ds' \frac{\mathcal{A}(s'-i\epsilon,t)}{(s'-s)}.$$

Provided $\mathcal{A}(s,t)$ falls to zero as $|s| \to \infty$, the contribution to the contour integration from the semi-circles at infinity may be neglected and using Eq.(1.3) we end up with the dispersion relation[†]

$$\mathcal{A}(s,t) = \frac{1}{\pi} \int_{s_{th}^+}^{\infty} \frac{\Im\mathrm{m}\mathcal{A}(s',t)}{(s'-s)} ds' + \frac{1}{\pi} \int_{-\infty}^{s_{th}^-} \frac{\Im\mathrm{m}\mathcal{A}(s',t)}{(s'-s)} ds'. \quad (1.9)$$

In the second of these integrals the imaginary part of the amplitude for $s < s_{th}^-$ is obtained from the Cutkosky rules applied to the u-channel process (1.7), i.e.

$$\Im\mathrm{m}\mathcal{A}(s < s_{th}^-, t) = -\Delta_u \mathcal{A}(s,t).$$

[†] We have assumed no contribution from bound state poles which generally add extra contributions.

https://doi.org/10.1017/9781009290111.003 Published online by Cambridge University Press

If the amplitude does *not* vanish as $|s| \to \infty$, then we have to make subtractions, i.e. we divide the amplitude by as many factors of $s - s_i$ as are necessary to produce a vanishing contribution from the semi-circles at infinity (the s_i are arbitrary and define the points at which the subtractions take place). For example, making one subtraction at $s = s_0$ we obtain the subtracted dispersion relation

$$\mathcal{A}(s,t) = \mathcal{A}(s_0,t) + \frac{(s-s_0)}{\pi}\int_{s_{th}^{+}}^{\infty} \frac{\Im\mathrm{m}\mathcal{A}(s',t)}{(s'-s)(s'-s_0)}\,ds' + \frac{(s-s_0)}{\pi}\int_{-\infty}^{s_{th}^{-}} \frac{\Im\mathrm{m}\mathcal{A}(s',t)}{(s'-s)(s'-s_0)}\,ds'. \qquad (1.10)$$

For our purposes we shall require the subtracted dispersion relation which allows us to reconstruct a function of s whose imaginary part is given by

$$A\,(\ln s)^n\,.$$

Equation (1.10) allows us to establish that, to leading order in $\ln s$, this function is purely real and equal to

$$-\frac{A}{(n+1)\pi}\,(\ln s)^{n+1}\,,$$

where we have used Eq.(1.3) to write

$$\ln(-s) = \ln(s) - i\pi.$$

Thus we see how, from three rather general postulates coupled with the spectrum of elementary particles, we can develop at least a set of self-consistency conditions for amplitudes and their relation to each other. Unitarity relates the imaginary parts of amplitudes to sums of products of other amplitudes, and dispersion relations then allow us to determine the corresponding real parts. The application of this process is called a **bootstrap** and it does not make any assumption about any underlying quantum field theory which may describe the dynamics of the strong interactions.

A further ingredient needed for the bootstrap is the asymptotic behaviour of amplitudes. Once we know these and their analytic structure then analyticity can be used to reconstruct the amplitudes. Determination of the asymptotic behaviour of amplitudes is the goal of Regge theory (Regge (1959, 1960)).

https://doi.org/10.1017/9781009290111.003 Published online by Cambridge University Press

1.2 Sommerfeld–Watson transform

Let us consider a two-particle to two-particle scattering process in the t-channel (Eq.(1.5)) at a centre-of-mass energy, $\sqrt{s}$, which is much larger than the masses of the external particles. The amplitude can be expanded as a series in Legendre polynomials, $P_l(\cos\theta)$, where θ is the (centre-of-mass frame) scattering angle and is related to s, t by

$$\cos\theta = 1 + \frac{2t}{s}.$$

This expansion is called the **partial wave expansion**, namely,

$$\mathcal{A}_{a\bar{c}\to\bar{b}d}(s,t) = \sum_{l=0}^{\infty}(2l+1)\,a_l(s)\,P_l\,(1+2t/s)\,. \tag{1.11}$$

$P_l(z)$ is a polynomial in z of degree l, and the functions $a_l(s)$ are called the **partial wave amplitudes.**

From the property of crossing symmetry (Eq.(1.6)) this may be continued into the s-channel by interchanging s and t to give

$$\mathcal{A}_{ab\to cd}(s,t) = \sum_{l=0}^{\infty}(2l+1)\,a_l(t)\,P_l\,(1+2s/t)\,. \tag{1.12}$$

Sommerfeld (1949), following Watson (1918), rewrote this partial wave expansion in terms of a contour integral in the complex angular momentum (l) plane as

$$\mathcal{A}(s,t) = \frac{1}{2i}\oint_C dl(2l+1)\frac{a(l,t)}{\sin\pi l}P(l,1+2s/t), \tag{1.13}$$

where the contour C surrounds the positive real axis as shown in Fig. 1.4. The Legendre polynomials can be expressed in terms of hypergeometric functions and analytically continued in l, giving the analytic function $P(l,z)$. The function $a(l,t)$ is an analytic continuation of the partial wave amplitudes $a_l(t)$. The denominator $\sin\pi l$ vanishes for integer l giving rise to poles which then reproduce Eq.(1.12).

1.3 Signature

It is now natural to ask if the function $a(l,t)$ is unique. At first sight it appears that it is not. For example we could add to $a(l,t)$ any analytic function which vanishes at integer values of

https://doi.org/10.1017/9781009290111.003 Published online by Cambridge University Press

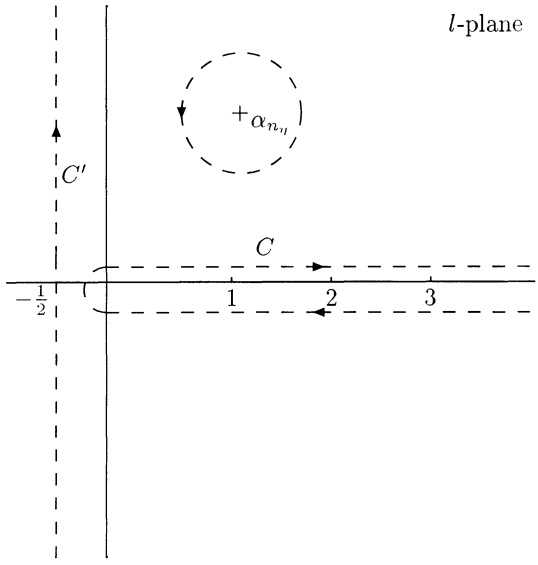

Fig. 1.4. Sommerfeld–Watson transform.

l without affecting the above result. However, using a theorem by Carlson (1914), it can be shown that $a(l,t)$ is unique provided $a(l,t) < \exp(\pi|l|)$ as $|l| \to \infty$. Unfortunately there are contributions to the partial wave amplitudes which alternate in sign, i.e. are proportional to $(-1)^l$ and so the required inequality is violated along the imaginary axis. It is therefore necessary to introduce *two* analytic functions $a^{(+1)}(l,t)$ and $a^{(-1)}(l,t)$ which are the analytic continuations of the even and odd partial wave amplitudes. Thus we have

$$\mathcal{A}(s,t) = \frac{1}{2i}\oint_C dl \frac{(2l+1)}{\sin \pi l} \sum_{\eta=\pm 1} \frac{(\eta + e^{-i\pi l})}{2} a^{(\eta)}(l,t)\, P(l, 1+2s/t), \tag{1.14}$$

where η, which takes the values ± 1, is called the **signature** of the partial wave and $a^{(+1)}(l,t)$ and $a^{(-1)}(l,t)$ are called the even- and odd-signature partial wave functions. The prefactors $\frac{1}{2}(\eta + \exp(-i\pi l))$ are called the signature factors.

https://doi.org/10.1017/9781009290111.003 Published online by Cambridge University Press

1.4 Regge poles

The next step is to deform the contour C of Fig. 1.4 to the contour C', which runs parallel to the imaginary axis with $\Re\mathrm{e}\, l = -\frac{1}{2}$. In order to do this we must encircle any poles or cuts that the functions $a^{(\eta)}(l,t)$ may have at $l = \alpha_{n_\eta}(t)$ and pick up $2\pi i \times$ the residue of that pole. For the particular case of simple poles only we arrive at

$$\mathcal{A}(s,t) = \frac{1}{2i}\int_{-\frac{1}{2}-i\infty}^{-\frac{1}{2}+i\infty} dl \left[\frac{(2l+1)}{\sin\pi l}\sum_{\eta=\pm 1}\frac{(\eta + e^{-i\pi l})}{2}a^{(\eta)}(l,t) \times P(l, 1+2s/t)\right] + \sum_{\eta=\pm 1}\sum_{n_\eta}\frac{(\eta + e^{-i\pi\alpha_{n_\eta}(t)})}{2}\frac{\tilde{\beta}_{n_\eta}(t)}{\sin\pi\alpha_{n_\eta}(t)}P(\alpha_{n_\eta}(t), 1+2s/t). \quad (1.15)$$

The simple poles $\alpha_{n_\eta}(t)$ are called even- ($\eta = +1$) and odd- ($\eta = -1$) signature **Regge poles** and $\tilde{\beta}_{n_\eta}(t)$ are the residues of the poles multiplied by $\pi(2\alpha_{n_\eta}(t)+1)$.

Throughout this book we shall be concerned with the **Regge region**, i.e. $s \gg |t|$. In this limit the Legendre polynomial is dominated by its leading term and we have

$$P_l(1+2s/t) \overset{s\gg|t|}{\longrightarrow} \frac{\Gamma(2l+1)}{\Gamma^2(l+1)}\left(\frac{s}{2t}\right)^l,$$

where $\Gamma(x)$ is the Euler gamma function. In this limit the contribution to the right hand side of Eq.(1.15) from the integral along the contour C' vanishes as $s \to \infty$, so that it may be neglected. It should now be clear why we exploited the crossing symmetry to write Eq.(1.12) and why we deformed the contour as in Fig. 1.4 – we wanted to exploit the asymptotic behaviour of the Legendre polynomial so as to isolate the high energy behaviour of the scattering amplitude in the Regge region. In fact we need only consider the contribution from the Regge pole with the largest value of the real part of $\alpha_{n_\eta}(t)$ (the leading Regge pole). Thus we have

$$\mathcal{A}(s,t) \overset{s\to\infty}{\longrightarrow} \frac{(\eta + e^{-i\pi\alpha(t)})}{2}\beta(t)s^{\alpha(t)}, \quad (1.16)$$

https://doi.org/10.1017/9781009290111.003 Published online by Cambridge University Press

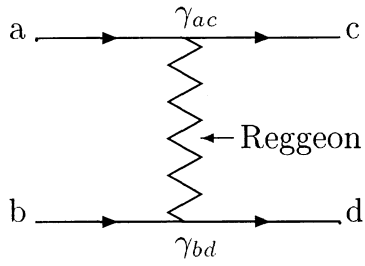

Fig. 1.5. A Regge exchange diagram.

where $\alpha(t)$ is the position of the leading Regge pole (at some value of t) and η is its signature. Some factors depending on t (but *not* on s) have been absorbed into the function $\beta(t)$.

Although we have assumed only simple poles in arriving at Eq.(1.16) it is possible that there are also non-simple poles and cuts which would lead to additional contributions to the amplitudes. We shall show that whereas the simple pole model works well for certain hadronic processes, leading logarithm perturbation theory can in general give rise to cuts.

1.5 Factorization

We can view the amplitude given by Eq.(1.16) as the exchange in the t-channel of an object with 'angular momentum' equal to $\alpha(t)$. This is of course not a particle since the 'angular momentum' is not integer (or half-integer) and it is a function of t. It is called a **Reggeon**. We can view a Reggeon exchange amplitude as the superposition of amplitudes for the exchanges of all possible particles in the t-channel. The amplitude can be factorized as shown in Fig. 1.5 into a coupling $\gamma_{ac}(t)$ of the Reggeon between particles a and c, a similar coupling $\gamma_{bd}(t)$ between particles b and d and a *universal* contribution from the Reggeon exchange. The couplings γ are functions of t only. Thus we obtain

$$\mathcal{A}(s,t) \overset{s\to\infty}{\longrightarrow} \frac{(\eta + e^{-i\pi\alpha(t)})}{2\sin\pi\alpha(t)} \frac{\gamma_{ac}(t)\gamma_{bd}(t)}{\Gamma(\alpha(t))} s^{\alpha(t)}. \tag{1.17}$$

We have explicitly extracted a factor of $\Gamma(\alpha(t))$ in defining the couplings γ. The reason for this is that if $\alpha(t)$ takes an inte-

https://doi.org/10.1017/9781009290111.003 Published online by Cambridge University Press

ger value for some value of t then the amplitude has a pole. For positive integers this can be understood as the exchange (in the t-channel) of a resonance particle with integer spin, but we would not expect such resonances with negative values of 'spin' . Such poles are called nonsense poles, and are cancelled by the factor $1/\Gamma(\alpha(t))$, which has zeroes at $\alpha(t) = 0, -1, -2 \cdots$.

One immediate consequence of Eq.(1.17) is the relation between the ρ-parameter, defined to be

$$\rho = \frac{\Re\mathrm{e}\,\mathcal{A}}{\Im\mathrm{m}\,\mathcal{A}}, \tag{1.18}$$

and the signature and position of the (leading) Regge pole. The couplings $\gamma_{ac}(t)$ and $\gamma_{bd}(t)$ are expected to be real functions of t and so from Eqs.(1.17) and (1.18) we have

$$\rho = -\frac{\eta + \cos\pi\alpha(t)}{\sin\pi\alpha(t)}. \tag{1.19}$$

1.6 Regge trajectories

If we consider the t-channel process, (1.5), with t positive we expect the amplitude to have poles corresponding to the exchange of physical particles of spin, J_i, and mass m_i, where $\alpha(m_i^2) = J_i$.

Chew & Frautschi (1961, 1962) plotted the spins of low lying mesons against square mass and noticed that they lie in a straight line as shown in Fig. 1.6. In other words $\alpha(t)$ is a linear function of t,

$$\alpha(t) = \alpha(0) + \alpha' t$$

(at least for positive t). From Fig. 1.6 we obtain the values

$$\begin{aligned} \alpha(0) &= 0.55 \\ \alpha' &= 0.86\ \mathrm{GeV}^{-2}. \end{aligned} \tag{1.20}$$

We shall see that this linearity continues for negative values of t.

From the s-dependence of the amplitude given in Eq.(1.17) we can deduce that the asymptotic s-dependence of the differential cross-section is given (for a linear trajectory) by

$$\frac{d\sigma}{dt} \propto s^{(2\alpha(0)-2\alpha' t-2)}. \tag{1.21}$$

https://doi.org/10.1017/9781009290111.003 Published online by Cambridge University Press

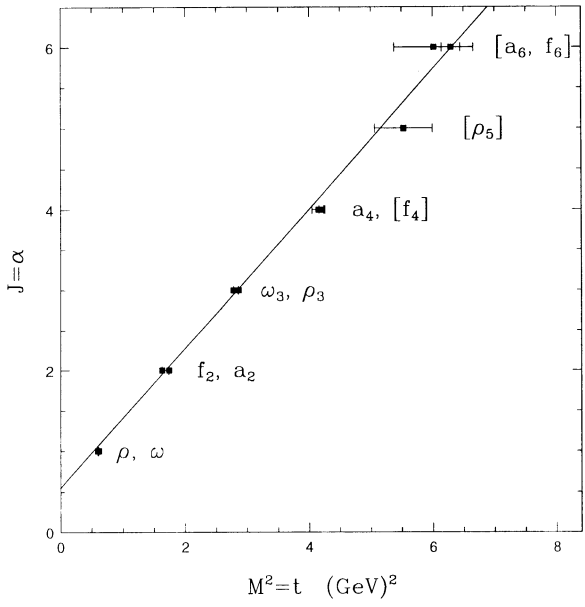

Fig. 1.6. The Chew–Frautschi plot.

If we consider a process in which isospin, $I = 1$, is exchanged in the t-channel, such as

$$\pi^- + p \rightarrow \pi^0 + n, \tag{1.22}$$

then we expect the Regge trajectory which determines the asymptotic s-dependence to be the one containing the $I = 1$ even parity mesons (the ρ-trajectory). Inserting the values Eq.(1.20) into Eq.(1.21) gives a very good fit to data over a wide range (20–200 GeV) of pion energies, as can be seen in Fig. 1.7.

The Regge trajectory has a further interesting feature. At $t = -0.64$ GeV^2 the trajectory passes through zero. This is an example of a nonsense pole (there cannot be a resonance with negative square mass) and, as explained above, it must decouple from the amplitude. The distinct dip observed in the differential cross-section for the process (1.22) plotted in Fig. 1.8 could well be evidence for the decoupling of this nonsense pole.

https://doi.org/10.1017/9781009290111.003 Published online by Cambridge University Press

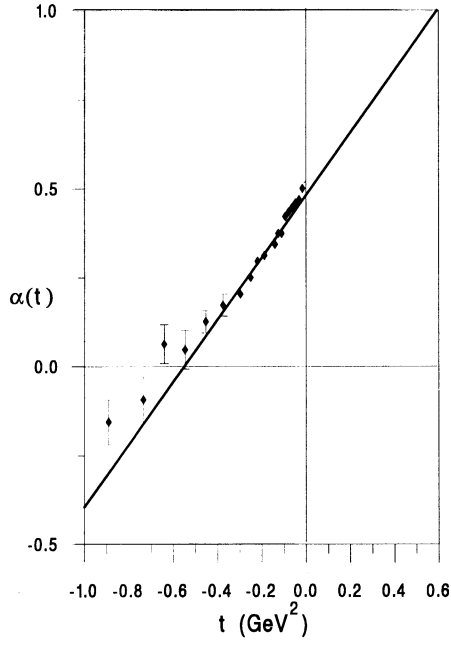

Fig. 1.7. $\alpha(t)$ obtained from $\pi^- p \to \pi^0 n$ data in the pion energy range 20.8–199.3 GeV by Barnes *et al.* (1976). The straight line is obtained by extrapolating the trajectory of Fig. 1.6 (see Eq.(1.20)).

1.7 The Pomeron

From the intercept of the Regge trajectory which dominates a particular scattering process and the optical theorem (Eq.(1.2)) we can obtain the asymptotic behaviour of the total cross-section for that process, namely,

$$\sigma_{\text{tot}} \propto s^{(\alpha(0)-1)}. \tag{1.23}$$

For the ρ-trajectory considered in the last section $\alpha(0) < 1$, which means that the cross-section for a process with $I = 1$ exchange falls as s increases.

Pomeranchuk (1956) and Okun & Pomeranchuk (1956) proved from general assumptions that in any scattering process in which

https://doi.org/10.1017/9781009290111.003 Published online by Cambridge University Press

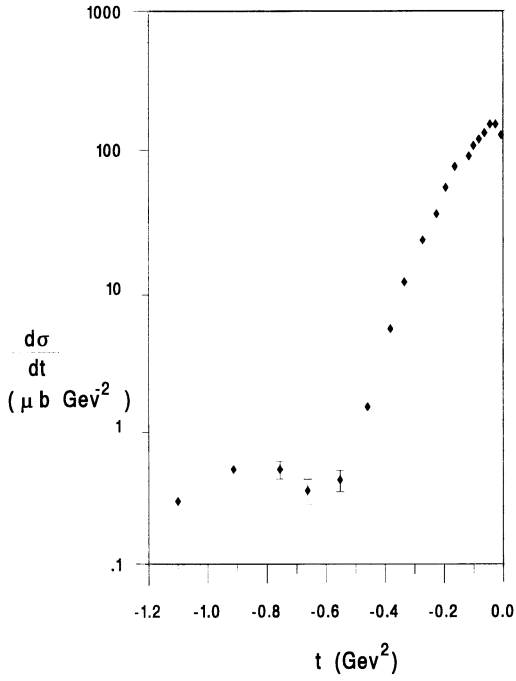

Fig. 1.8. Data on $d\sigma/dt$ for the process $\pi^- p \to \pi^0 n$ at a beam energy of 20.8 GeV from Barnes *et al.* (1976). The differential cross-section has a dip at $t \approx -0.6$ GeV^2.

there is charge exchange the cross-section vanishes asymptotically (the Pomeranchuk theorem). Foldy & Peierls (1963) noticed the converse, namely, that if for a particular scattering process the cross-section does *not* fall as s increases then that process must be dominated by the exchange of vacuum quantum numbers (i.e. isospin zero and even under the operation of charge conjugation).

It is observed experimentally that total cross-sections do not vanish asymptotically. In fact they rise slowly as s increases. If we are to attribute this rise to the exchange of a single Regge pole then it follows that the exchange is that of a Reggeon whose intercept, $\alpha_P(0)$, is greater than 1, and which carries the quantum

https://doi.org/10.1017/9781009290111.003 Published online by Cambridge University Press

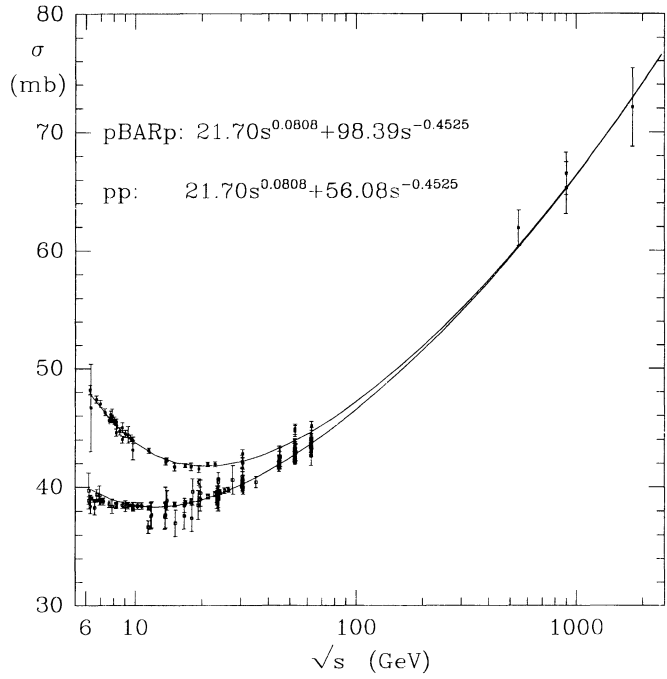

Fig. 1.9. Data for p–p and p–$\bar{p}$ total cross-sections and the fit of Eq.(1.24).

numbers of the vacuum.† This trajectory is called the **Pomeron** and is named after its inventor Pomeranchuk (1958).

Unlike the Regge trajectory of Fig. 1.6 the physical particles which would provide the resonances for integer values of $\alpha_P(t)$ for positive t have not been conclusively identified. Particles with the quantum numbers of the vacuum are difficult to detect, but such particles can exist in QCD as bound states of gluons (glueballs).

1.8 Total cross-sections

Fig. 1.9 shows a compilation of data for the total cross-sections

† The particles with $I = 0$ shown on the trajectory in Fig. 1.6 do *not* have the quantum numbers of the vacuum since they are odd under charge conjugation.

https://doi.org/10.1017/9781009290111.003 Published online by Cambridge University Press

for proton–proton (p–p) and proton–antiproton (p–$\bar{p}$) scattering, together with a fit due to Donnachie & Landshoff (1992):

$$\begin{aligned} \sigma_{pp} &= 21.7\, s^{0.08} + 56.1\, s^{-0.45} \text{ mb} \\ \sigma_{\bar{p}p} &= 21.7\, s^{0.08} + 98.4\, s^{-0.45} \text{ mb} \end{aligned} \tag{1.24}$$

(with s in GeV^2). These parameters were determined *before* the measurement of the p–p cross-section at the Fermilab Tevatron accelerator (from fitting to a wide range of data below $\sqrt{s}$ =100 GeV).

The first term on the right hand side of Eq.(1.24) is the Pomeron contribution and it is common to both p–p and p–$\bar{p}$ cross-sections, coupling with the same strength to the proton and antiproton because the Pomeron carries the quantum numbers of the vacuum and therefore cannot distinguish between particles and antiparticles. The second term, on the other hand, is a sub-leading term which is due to the exchange of a Regge trajectory with intercept 0.55 (the intercept of the Regge trajectory shown in Fig. 1.6) and this trajectory can (and does) have different couplings to particles and antiparticles. This accounts for the difference between the p–p and p–$\bar{p}$ cross-sections at low s (this difference vanishes as s increases by the Pomeranchuk theorem).

This fit tells us that the Pomeron has intercept $\alpha_P(0) = 1.08$. This is slightly above 1 and will eventually lead to a violation of the bound derived by Froissart (1961) and Martin (1963) which is derived using unitarity and the partial wave expansion (we present a physical argument for the Froissart–Martin bound in Chapter 8). They showed that, as s tends to infinity, total hadronic cross-sections must satisfy the inequality

$$\sigma_{\text{tot}} < A \ln^2 s, \tag{1.25}$$

where the constant A is determined by the pion mass and is expected to be $\sim$ 60 mb. However, since the intercept is only very slightly above 1, this violation does not occur for momenta lower than the Planck scale! It is not unreasonable that physics beyond the exchange of the single Pomeron pole enters to ensure the ultimate preservation of unitarity (in fact it is known that multiple Pomeron exchanges are able to tame the asymptotic rise of the cross-section). Another point of view is to argue that the intercept of 1.08 is only an effective intercept and that the underlying mechanism which gives rise to it is not the result of single

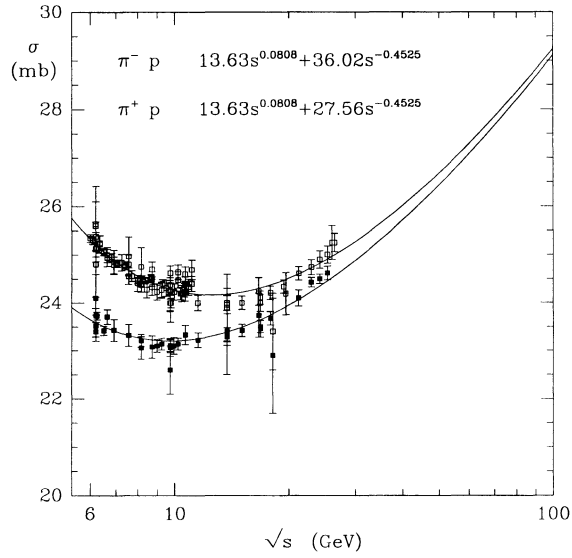

Fig. 1.10. Total cross-sections for π^+–p and π^-–p scattering.

Pomeron exchange but has contributions from the exchange of two or more Pomerons (so-called **Regge cuts**).

If the high energy behaviour of the total cross-section is indeed a result of the superposition of the two Regge exchanges, with intercepts as quantified in Eq.(1.24), then since the intercepts are universal we expect them to be able to describe other total cross-sections. This is indeed the case, as can be seen from Fig. 1.10 for the case of pion–proton scattering and Fig. 1.11 for (on-shell) photon–proton scattering.

1.9 Differential elastic cross-sections

In order to determine the slope, α'_P, of the Pomeron trajectory it is necessary to consider the differential cross-section, e.g. for elastic p–p or p–$\bar{p}$ scattering, over a range of s and at different values of t. A collection of data ranging from ISR at CERN to the Tevatron at Fermilab give a good fit to a linear Pomeron trajectory with

https://doi.org/10.1017/9781009290111.003 Published online by Cambridge University Press

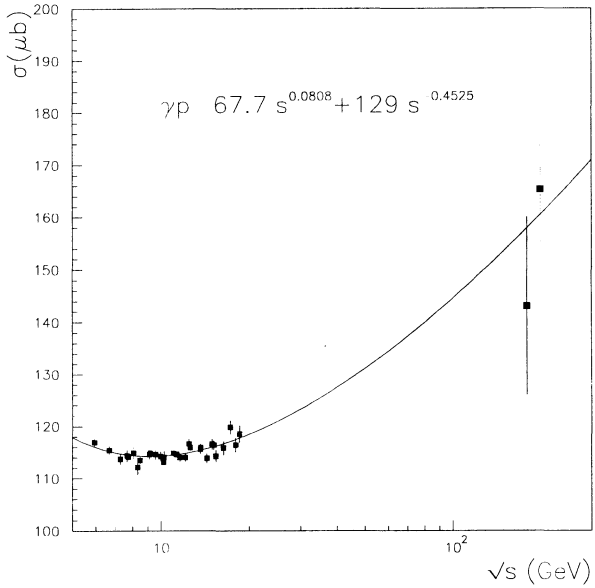

Fig. 1.11. The cross-section for γ–p scattering.

slope

$$\alpha'_P = 0.25 \text{ GeV}^{-2}.$$

From this slope we can determine that $\alpha_P(t)$ reaches the value 2 at $t = 3.7$ GeV^2 and we should expect a spin two particle with mass $\sqrt{3.7} = 1.9$ GeV and the quantum numbers of the vacuum. The WA91 collaboration at CERN (Abatzis *et al.* (1994)) has announced evidence for a candidate glueball state with this mass. This could well be the first observed particle to lie on the Pomeron trajectory.

The couplings, $\gamma(t)$, of the Pomeron can also be obtained from the t-dependence of differential elastic cross-sections (at fixed s). It turns out that the data are well fitted by taking the Pomeron coupling $\gamma(t)$ to be proportional to the electromagnetic form factor of the hadron to which the Pomeron couples. In other words the Pomeron couples to hadrons in the same way as the photon. Thus when the Pomeron couples to hadrons it appears to behave like a point particle. One immediate consequence of this, as was noted

https://doi.org/10.1017/9781009290111.003 Published online by Cambridge University Press

by Landshoff & Polkinghorne (1971), is the quark-counting rule which tells us that the Pomeron couples to one constituent quark at a time inside a hadron, so that the coupling to that hadron is expected to be proportional to the number of valence quarks. This quark-counting rule is well supported by the fact that the coefficients of the Pomeron term in the fits to p–p and π–p scattering are in the ratio 1.6:1, which is just slightly higher than the ratio 3:2 that would be expected from the fact that the proton has three valence quarks whereas the pion has only two.

The ρ-parameter (Eq.(1.18)) can also be obtained from the differential elastic cross-section at zero momentum transfer and the total cross-section. The former is proportional to the sum of the squares of the real and imaginary parts of the scattering amplitude, whereas the latter is related by the optical theorem to the imaginary part of the amplitude. Thus we have

$$\frac{d\sigma^{\mathrm{el}}(s,0)}{dt} = \frac{(1+\rho^2)}{16\pi}|\sigma_{\mathrm{tot}}|^2. \tag{1.26}$$

Experimental values such as those of Augier *et al.* (1993) from the UA4 collaboration at CERN give a value of ρ of about 0.1 at $\sqrt{s} \approx 100$ GeV. In other words the amplitude for Pomeron exchange is dominated by its imaginary part. From the fact that the intercept of the Pomeron is close to 1 and Eq.(1.19) we can deduce that the Pomeron must have even signature ($\eta = 1$).

1.10 Diffractive dissociation

At sufficiently high energies elastic-scattering events are rather difficult to detect since the particles scatter through small angles. However, the Pomeron enters into several other processes. One of these is the process of diffractive dissociation in which one of the incident particles remains unchanged and just scatters through a small angle, but the other incident particle receives enough energy for it to break up into its constituent partons, which then hadronize to produce clusters of hadrons.

It is convenient to view such a process from the point of view suggested by Fig. 1.12, where a Pomeron is 'emitted' from the 'parent' hadron (with momentum p_2 and which remains intact after the scattering) with some fraction ξ of its momentum. The

https://doi.org/10.1017/9781009290111.003 Published online by Cambridge University Press

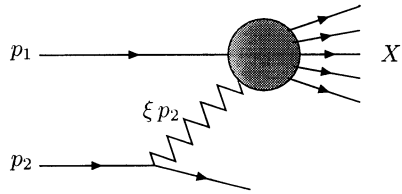

Fig. 1.12. A diffractive dissociation process in which the exchanged Pomeron carries a fraction ξ of the momentum p_2 of one of the incoming hadrons.

upper vertex can be thought of as 'hadron–Pomeron' scattering producing some final hadronic state, X.

Such events have a large **rapidity gap** between the 'parent' hadron and the hadrons in the hadronic system, X. The rapidity, y_i, of particle i is defined as

$$y_i = \frac{1}{2}\ln\left(\frac{E_i + p_{zi}}{E_i - p_{zi}}\right),$$

where the z-axis is taken along the incident beam direction. Since the scattering angle is small ($|t|$ is much smaller than s) the 'parent' hadron emerges almost along the positive z-axis and therefore has large positive rapidity, whereas the particles in the hadronic system X are moving almost parallel to the negative z-axis (the momentum transfer between the target hadron and the particles in X is small) and they therefore have large negative rapidities.

Events of this kind have been observed by the UA8 collaboration at CERN (Schlein (1993)) and by the H1 (Ahmed *et al.* (1994, 1995a)) and Zeus (Derrick *et al.* (1993, 1995a)) collaborations at DESY. UA8 have measured the energy flow of the particles in the hadronic system X in its rest frame (i.e. the centre-of-mass frame of the hadron–Pomeron system) and observed a substantial peak in the forward direction. This once again suggests that the Pomeron can behave like a point particle, knocking the constituents of the target hadron into the forward direction.

Although the Pomeron seems to behave as though it were a point-like particle, we must remember that it is not a particle at all. It is a Regge trajectory. Nevertheless Ingelman & Schlein (1985) suggested that one can define the structure function of a Pomeron and use diffractive dissociation events to determine the

quark and gluon content of the Pomeron. Furthermore, the substructure of the Pomeron has been investigated by the H1 (Ahmed *et al.* (1995b)) and Zeus (Derrick *et al.* (1995b, 1996a)) collaborations.

We shall return to discuss the theory of diffraction dissociation in much more detail in Chapter 7.

1.11 Deep inelastic scattering

The measurement of structure functions ($F_1(x, Q^2)$ and $F_2(x, Q^2)$) in deep inelastic scattering can be thought of as the measurement of the total cross-section for the scattering of an off-shell photon, with square momentum, $-Q^2$, and a proton. The square of the centre-of-mass energy of the photon–proton system is given by

$$s = \frac{Q^2(1-x)}{x}$$

and so in the Regge limit of $s \gg Q^2$ it follows that $x \ll 1$ (x is the Bjorken-x of the process). At sufficiently low x the off-shellness of the photon is negligible compared with the centre-of-mass energy and so we might expect the total cross-section to have a $1/x$ dependence (at fixed Q^2) similar to the s-dependence of hadronic total cross-sections, i.e. governed by Pomeron exchange. Adding the lower lying meson trajectory, we would then have

$$F_2(x, Q^2) \overset{x \to 0}{\longrightarrow} A\, x^{-0.08} + B\, x^{0.45}.$$

This fits well for $0.01 \lesssim x \lesssim 0.1$. However, the H1 (Ahmed *et al.* (1995c)) and Zeus (Derrick *et al.* (1995c)) collaborations at HERA have been able to reach values as low as $x \sim 10^{-4}$. The data they obtain show a much steeper x-dependence, e.g. typically $\sim x^{-0.3}$. These data provide, for the first time, evidence of deviations from the Pomeron behaviour described previously.

As we shall see, such deviations are expected within QCD perturbation theory. The large virtuality Q^2 renders a perturbative calculation possible. In Chapter 6 we shall show that perturbative QCD leads to the conclusion that, at sufficiently large Q^2 and sufficiently low x, the structure functions ought to behave like

$$\sim x^{-\omega_0},$$

https://doi.org/10.1017/9781009290111.003 Published online by Cambridge University Press

where

$$\omega_0 = \frac{12\ln 2}{\pi}\alpha_s,$$

and α_s is the strong coupling.

On the other hand, total hadronic cross-sections or low t elastic differential cross-sections cannot be described in terms of perturbative QCD. We expect these processes to be heavily influenced by the non-perturbative properties of QCD, i.e. the Pomeron discussed in this chapter is of non-perturbative origin. We call this the 'soft' Pomeron since in later chapters we shall introduce the concept of the perturbative or 'hard' Pomeron. These are distinct objects. In keeping with modern parlance we use the word 'Pomeron' (soft or hard) in the context of those processes which are characterized by the kinematic condition that the momentum transfer is much smaller than the centre-of-mass energy and in which the vacuum quantum numbers are exchanged.

In future we shall end each chapter with a summary. However, this chapter has been a summary in itself. It has been designed to give the reader sufficient understanding of what we mean when we speak of the Pomeron and why it is an important object. This will be necessary in order to progress through the subsequent chapters, in which we will discuss in detail the question of the reconciliation of Pomeron physics with the 'modern' approach to strong interaction dynamics – namely QCD.